^{18}F-Dihydroxyphenylalanine PET in Patients with Biochemical Evidence of Medullary Thyroid Cancer: Relation to Tumor Differentiation

Klaas P. Koopmans[1], Jan Willem B. de Groot[2], John T.M. Plukker[3], Elisabeth G.E. de Vries[4], Ido P. Kema[5], Wim J. Sluiter[2], Pieter L. Jager[1], and Thera P. Links[2]

[1]Departments of Nuclear Medicine and Molecular Imaging, University Medical Center Groningen, Groningen, The Netherlands; [2]Department of Endocrinology, University Medical Center Groningen, Groningen, The Netherlands; [3]Department of Surgical Oncology, University Medical Center Groningen, Groningen, The Netherlands; [4]Department of Medical Oncology, University Medical Center Groningen, Groningen, The Netherlands; and [5]Department of Pathology and Laboratory Medicine, University Medical Center Groningen, Groningen, The Netherlands

Curative treatment for recurrent medullary thyroid cancer (MTC), diagnosed by rising serum calcitonin, is surgery, but tumor localization is difficult. Therefore, the value of ^{18}F-dihydroxyphenylanaline PET (^{18}F-DOPA PET), ^{18}F-FDG PET, ^{99m}Tc-V-di-mercaptosulfuricacid (DMSA-V) scintigraphy, and MRI or CT was studied. **Methods:** Twenty-one patients with biochemical recurrent or residual MTC underwent ^{18}F-DOPA PET, ^{18}F-FDG PET, DMSA-V scintigraphy, and MRI or CT. Patient- and lesion-based sensitivities were calculated using a composite reference consisting of all imaging modalities. **Results:** In 76% of all patients with MTC, one or more imaging modalities was positive for MTC lesions. In 6 of 8 patients with a calcitonin level of <500 ng/L, imaging results were negative. In 15 patients with positive imaging results, ^{18}F-DOPA PET detected 13 (sensitivity, 62%; with 4.6 lesions per patient [lpp]). Morphologic imaging (n = 19) was positive in 7 (sensitivity, 37%; 4.7 lpp), DMSA-V (n = 18) in 5 (sensitivity, 28%; 1.1 lpp), and ^{18}F-FDG PET (n = 17) in 4 (sensitivity, 24%; 1.6 lpp). In a lesion-based analysis, ^{18}F-DOPA PET detected 95 of 134 lesions (sensitivity, 71%), morphologic imaging detected 80 of 126 (sensitivity, 64%), DMSA-V detected 20 of 108 (sensitivity, 19%), and ^{18}F-FDG PET detected 48 of 102 (sensitivity, 30%). In 2 of 3 patients with a calcitonin/carcinoembryonic antigen (CEA) doubling time of ≤12 mo, ^{18}F-FDG PET performed better than ^{18}FDOPA PET; in the third patient, ^{18}F-FDG PET was not performed. **Conclusion:** MTC lesions are best detectable when serum calcitonin was >500 ng/L. ^{18}F-DOPA PET is superior to ^{18}F-FDG PET, DMSA-V, and morphologic imaging. With short calcitonin doubling times (≤12 mo), ^{18}F-FDG PET may be superior.

Key Words: medullary thyroid cancer; PET; ^{18}F-DOPA; ^{18}F-FDG; tumor markers; tumor differentiation; calcitonin

J Nucl Med 2008; 49:524–531
DOI: 10.2967/jnumed.107.047720

Medullary thyroid carcinoma (MTC) originates from the parafollicular C-cells of the thyroid. It accounts for 3%–10% of all thyroid malignancies (*1*). Because C cells produce calcitonin, this hormone serves as a reliable tumor marker for MTC. Another frequently used marker is carcinoembryonic antigen (CEA) (*1,2*). Calcitonin doubling time can be helpful in the judgment of the clinical course (*3,4*), although the transition to progressive disease with overt metastases is often unpredictable.

Thus far, surgery consisting of a total thyroidectomy and extensive lymph node dissection is the only effective curative treatment (*5–8*) in primary MTC. However, after clinical curative surgery, biochemical cure rates vary from 34% to 44%. Again, the only curative treatment option in these patients with residual or recurrent disease after initial treatment is further surgery. However, surgery can be successful only when the surgeon is accurately informed about the location of local and distant metastases and usually only when residual or recurrent MTC is confined to the neck.

Therefore, it is important to identify the source of the increased calcitonin as early as possible. However, the source of calcitonin production is hard to identify with conventional medical imaging and therefore distant metastases cannot be reliably ruled out. ^{18}F-FDG PET and ^{99m}Tc(V) dimercaptosuccinic acid scintigraphy (DMSA-V) have reasonable sensitivity for the detection of MTC metastases. However, in about half of the patients, persistent MTC cannot be detected with any morphologic (CT or MRI) or functional imaging (^{18}F-FDG PET, DMSA-V, or ^{111}In-octreotide scintigraphy) (*4,9,10*).

Apart from the problematic restaging, another clinical problem is the unpredictable clinical course in patients with persistent disease. Although the overall survival of patients with biochemical detectable disease is relatively long, the transition to progressive disease is often unpredictable (*3*). Early detection of such an accelerated phase might lead to

Received Oct. 3, 2007; revision accepted Dec. 13, 2007.
For correspondence contact: Thera P. Links, MD, PhD, Department of Endocrinology, University Medical Centre Groningen, P. O. Box 30.001, 9700 RB Groningen, The Netherlands
E-mail: t.p.links@int.umcg.nl.

better treatment and, for this purpose serum, calcitonin doubling time has proven to be valuable (*3,4*).

^{18}F-Dihydroxyphenylanaline (^{18}F-DOPA) PET is a new functional nuclear medicine procedure that enables metabolic imaging of MTC. This approach is based on the increased activity of large amino acid transporter (LAT) systems in neuroendocrine tumors such as MTC (*11*). The first reports of the use of ^{18}F-DOPA PET in patients with MTC are promising but included only a very small number of patients (*12,13*). The aim of the present study was to assess the value of ^{18}F-DOPA PET in patients with elevated calcitonin and CEA levels in comparison with the results with ^{18}F-FDG PET, DMSA-V, and morphologic imaging (CT or MRI). The secondary aim was to evaluate whether there was a relation between the level and the course of tumor markers and imaging results.

MATERIALS AND METHODS

Patients

Patients who had histologically proven MTC and elevated serum calcitonin levels after initial surgical treatment were eligible for this prospective single-center study. They were included between January 2003 and March 2007. The local medical ethics committee approved the study, and all patients gave written informed consent.

Imaging Protocol

According to our protocol, all patients with recurrent or residual MTC, diagnosed by elevated serum calcitonin or CEA or chromogranin A levels, underwent ^{18}F-DOPA PET, DMSA-V scintigraphy, ^{18}F-FDG PET, and morphologic imaging with CT or MRI. DMSA-V and ^{18}F-FDG PET were not performed when such scans had been made repeatedly with negative results in the previous 2 y. The regions of metastasis or recurrence were divided into 5 areas: regional, lung, liver abdomen and bone.

^{18}F-FDG PET, DMSA-V scintigraphy, and morphologic imaging were performed as described previously (*9*). These scans were interpreted by dedicated specialists as part of routine patient care and subsequently were independently reread.

^{18}F-DOPA PET

^{18}F-DOPA was locally produced as described earlier (*14*). Patients fasted for 6 h before examination and were allowed to continue all medication. Whole-body 2-dimensional PET images were acquired 60 min after intravenous administration of ^{18}F-DOPA (180 ± 50 MBq), on an ECAT HR+ positron camera (Siemens Medical Solutions, Inc.) with attenuation correction (7–10 bed positions of 5-min emission and 3-min transmission scans; total scanning time, approximately 60 min). For the reduction of tracer decarboxylation and subsequent renal clearance all patients received 2 mg/kg carbidopa orally as pretreatment 1 h before the ^{18}F-DOPA injection to increase tracer uptake in tumor cells (*15–17*).

Two nuclear medicine physicians interpreted the ^{18}F-DOPA PET images independently. These readers were unaware of calcitonin, CEA, and chromogranin A levels and the results of other imaging examinations. Only lesions in each body region with an unequivocal visibility clearly above normal activity, known from patients and regions without tumors, were considered abnormal.

Composite Reference Standard

As a composite reference standard for the presence of tumor lesions, all available cytologic, histologic, follow-up findings and all imaging findings were used (*18*). In these patients, cytologic or histologic verification of every lesion is neither feasible nor justifiable. Histologic confirmation of disease would be the ideal verification of tumor activity, but for obvious reasons surgery or biopsy of all lesions on the combined imaging methods is not feasible. Whenever possible, new findings were verified with additional other investigations, such as ^{111}In-octreotide scintigraphy (n = 3), meta-iodobenzylguanidine (MIBG) (n = 3), bone scintigraphy (n = 1), and surgical findings (n = 5).

Biochemical Analysis

As markers for tumor activity we measured serum calcitonin levels (reference values, 0.3–12 ng/L) by enzyme-linked immunosorbent assay (Sangui Biotech Inc.) and plasma CEA levels (reference values, 0.5–5.0 μg/L), which were measured by chemilumnescent microparticle immunoassay (Abbott Laboratories). Serum chromogranin A was determined using a radioimmunoassay (Cga-React; Cis Bio International) as a marker for tumor volume (reference values, 20.0–100.0 mg/L). The formula $\log 2 \times dT/(\log B - \log A)$ was used to estimate the calcitonin and the CEA doubling time. In this formula, A is the initial concentration and B is the following calcitonin or CEA concentration. dT is the time difference between the measurements of A and B in months (*19*).

Data and Statistical Analysis

Because all patients presented with elevated serum calcitonin levels, any imaging study not showing a clear abnormality was classified as false-negative in the patient-based analysis. In addition, region- and lesion-based sensitivities were calculated using the composite reference standard and were compared using paired observations and the McNemar test. Patient-based sensitivity was calculated as the number of patients with a positive test (at least 1 lesion detected) by the total number of patients in whom the test was performed. Regional sensitivity was calculated by dividing the number of regions positive for tumor detected by that modality by the total number of tumor-positive regions (composite reference), and the lesion-based sensitivity was calculated by dividing the number of detected lesions by the total number of lesions (composite reference). For the patient-based analysis, the McNemar test was used to compare ^{18}F-DOPA PET findings with those from ^{18}F-FDG PET, ^{99m}Tc-DMSA-V, and morphologic imaging. To compare the number of patients with 0, 1, 2, 3, or more positive regions between ^{18}F-DOPA PET and the other imaging modalities, the Pitman test was used. These tests were not corrected for multiple testing. For the comparison of number of lesions per region, the Wilcoxon test was used. The χ^2 test was used to compare proportions of abnormal biochemical markers in positive and negative imaging. The significance level was 0.05, 2-sided. Confidence intervals are given in the tables. The statistical tests were performed using the SPSS package 12.0.

RESULTS

Twenty-one consecutive patients (10 men and 11 women) were included. Twelve patients had sporadic MTC, 8 had multiple endocrine neoplasia (MEN) syndrome type 2A, and 1 had MEN 2B. All diagnostic imaging examinations of the same patient were completed within a 9-mo interval, which

was always relatively short in comparison with the rate of disease progression, The examinations were performed at least 4 mo after any therapy. ^{18}F-FDG PET was obtained on 18 patients, DMSA-V scintigraphy on 19 patients, and MRI or CT of the neck and mediastinum on 18 patients. In the other patients such scans had been made repetitively in the previous 2 y with negative results. All of these patients underwent the imaging procedures after initial total thyroidectomy with central compartment dissection and additional neck dissection if indicated. Laparoscopy for detection of minimal, capsular liver disease was not part of the standard dissemination strategy. The median age was 52 y (range, 19–75 y). Clinical characteristics of the individual patients are listed in Table 1.

Imaging Results

Patient-Based Analysis. ^{18}F-DOPA PET produced high-quality tomographic images that were easily interpretable (Fig. 1). In 6 patients (29%) no lesions could be detected with either of the imaging methods used; these were therefore classified as false-negative. Table 2 summarizes the imaging results per patient. Although morphologic imaging methods were able to detect a slightly larger number of tumor lesions per positive patient (patient-based sensitivity, 39%; 4.7 lesions per patient [lpp]), ^{18}F-DOPA PET was able to detect 13 tumor-positive patients (patient-based sensitivity, 62%; 4.6 lpp). DMSA-V and ^{18}F-FDG PET detected considerably fewer tumor lesions. DMSA-V detected 5 and ^{18}F-FDG PET detected 4 tumor-positive patients (sensitivity of 26% for DMSA-V vs. 22% for ^{18}F-FDG PET, 1.1 lpp vs. 1.6 lpp). DMSA-V and ^{18}F-FDG PET were both positive in 1 patient but detected different lesions. However, because of the small number of patients, no statistically significant difference in the patient-based analysis could be reached between the described imaging methods. In 4 patients, surgery was performed as a result of ^{18}F-DOPA PET findings. In these patients, the lesions detected with ^{18}F-DOPA PET were resected and proven to be tumor-positive on pathologic analysis.

Region-Based Analysis. Table 3 describes the region-based analysis. Of the 126 regions evaluated, 37 (29%) were considered positive for tumor. ^{18}F-DOPA PET detected 33 of these positive regions (sensitivity, 89%), whereas morphologic imaging detected 17 positive regions (sensitivity, 52%), DMSA-V scintigraphy detected 9 positive regions (sensitivity, 33%), and ^{18}F-FDG PET detected 12 (sensitivity, 48%).

Lesion-Based Analysis. A total of 134 lesions were considered positive for tumor on the basis of the composite reference standard. ^{18}F-DOPA PET detected 95 of 134 (sensitivity, 71%) lesions. The sensitivity of ^{18}F-DOPA PET was higher than that of morphologic imaging in which both were performed ($P = 0.019$). Morphologic imaging detected 80 of 126 lesions (sensitivity, 64%). DMSA-V and ^{18}F-FDG were inferior to ^{18}F-DOPA PET, as DMSA-V detected only 20 of 108 (sensitivity, 19%; $P = 0.031$ for paired comparison of ^{18}F-DOPA PET with DMSA-V) and ^{18}F-FDG PET detected only 48 of 102 (sensitivity, 30%; $P = 0.123$ for paired comparison of ^{18}F-DOPA PET with ^{18}F-FDG PET) (Table 3). Most lesions were present in the liver and bone (liver, 41; bone, 27). ^{18}F-DOPA PET showed more lesions in the liver region (47 for ^{18}F-DOPA PET vs. 28 for CT or MRI); however, morphologic imaging methods were able to detect more bone lesions (27 for CT/MRI vs. 8 for ^{18}F-DOPA PET). The combination of CT or MRI, DMSA-V, and ^{18}F-FDG PET results in a total of 90 lesions (sensitivity, 71%), which is still slightly less than the number of lesions detected by ^{18}F-DOPA PET alone.

Comparison of Imaging with Calcitonin

All patients had elevated serum calcitonin levels (median, 1,064 ng/L; range, 24–120,000 ng/L). Using an arbitrary calcitonin threshold of 500 ng/L (*4*), 12 of the 13 patients with serum calcitonin levels higher than 500 ng/L had positive ^{18}F-DOPA PET scans ($P = 0.002$ for comparison of positive scan results vs. calcitonin $>$ 50 ng/L). Of the 8 patients with a serum calcitonin level below 500 ng/L, 6 had negative imaging results. One patient (patient 10) had a lesion lateral to the right side of the urinary bladder lesion, which was present only on ^{18}F-DOPA PET. This patient had normal CEA levels, and the median calcitonin doubling time was 27 mo (range, 4–108 mo).

After combining a calcitonin level of $>$500 ng/L with a calcitonin doubling time of $>$12 mo as the classification of biochemically active but slowly progressive MTC, we evaluated 10 patients. ^{18}F-DOPA PET was positive in 9 patients. In 7 of these 10 patients ^{18}F-DOPA PET detected more lesions than the other imaging modalities; in 3 patients ^{18}F-DOPA PET detected the same lesions as the other imaging modalities, and in patient 21 (with doubling time just over 12 mo) ^{18}F-DOPA PET revealed an additional abdominal lesion that was not evident on all other imaging modalities but failed to identify a thoracic lesion that was identified by ^{18}F-FDG PET. In contrast, ^{18}F-FDG PET was negative in 6 of 7 patients with a calcitonin level of $>$500 ng/L and a calcitonin doubling time of $>$12 mo. In 1 patient (patient 21), ^{18}F-FDG PET detected an additional thoracic lesion but failed to identify 1 abdominal lesion that was detected by ^{18}F-DOPA PET. Two patients (patients 4 and 5) were exceptional: They had very high CgA and calcitonin levels but a long doubling time for both. Contrary to ^{18}F-DOPA PET and CT, ^{18}F-FDG PET was negative in these 2 patients. These doubling times and the clinical behavior suggest a slow-growing tumor with a low-glucose need in these patients.

A calcitonin level of $>$500 ng/L and a calcitonin doubling time of $<$12 mo as the characterization of biochemically active and rapidly progressing tumor was present 3 patients (Fig. 2). These 3 patients (patients 2, 12, and 18) have died since entering the study. Patients 2 and 18 had more ^{18}F-FDG PET-positive lesions then ^{18}F-DOPA PET-positive lesions. Unfortunately, because of progressive disease, patient 12 did not undergo ^{18}F-FDG PET scanning.

TABLE 1
Patient Characteristics of Study Population

Patient no	Age (y)	Sex	Type MTC	CgA (mg/L)	Calcitonin (ng/L)	Calcitonin doubling time (mo)	CEA μg/L	CEA doubling time (mo)	CT or MRI	DMSA-V	^{18}F-FDG PET	^{18}F-F-DOPA PET	Imaging performance or histologic confirmation
1	71	M	spor	58	418	53	5.2	143	Neg	Neg	Neg	Neg	−/N
2*	**56**	**F**	**MEN 2a**	**32**	**10,500**	**8**	**414.8**	**9**	**Li5; os2**	**Neg**	**he1; li2; os2**	**li2; os2**	**−/N**
3	66	M	spor	37	825	13	7.3	247	Neg	Neg	Neg	ab1	++
4	71	M	spor	466	120,000	24	2,209.5	29	Li8; os10	Neg	Neg	li10; os2	+
5	68	F	MEN 2a	200	27,190	91	1,459.5	151	Li10; os5	ne3; th1; li4;os1	Neg	he1; ne3; th1; li10; os1	+
6	48	M	MEN 2b	147	1,080	61	32.5	103	Neg	Neg	Neg	ne1	+/Y
7	56	M	MEN 2a	35	48	43	1.4	268	N/P	Neg	Neg	Neg	−/N
8	27	F	MEN 2a	23	73	29	1.2	77	Neg	os2	ne1	Neg	—/N
9	52	M	spor	77	173	34	14	−46	Neg	Neg	Neg	Neg	−/N
10	43	F	MEN 2a	28	86	76	1.1	−40	Neg	Neg	Neg	ab1	+/N
11	59	F	spor	56	1,596	−22	30.3	56	He1; ne2	N/P	N/P	he1; ne2	−/N
12*	**57**	**M**	**spor**	**910**	**109,000**	**8**	**647.1**	**15**	**He1; ne1; th10; li5**	**N/P**	**N/P**	**he1; ne2; th10; li8**	**+/Y**
13	48	F	MEN 2a	82	112	−43	0.5	232	N/P	Neg	Neg	Neg	−/N
14	78	M	MEN 2a	147	2,812	27	3.4	−108	Ne1; th5	ne1	N/P	ne1; th3; li1	+/Y
15	34	F	spor	26	4,600	29	9.8	−42	Neg	N/P	N/P	ne1	+/Y
16	72	F	MEN 2a	120	19,350	68	194.3	−98	Neg	Neg	Neg	ne1; th1; li10	++
17	45	M	spor	284	1,049	108	29.5	50	Neg	h1	Neg	Neg	—/N
18*	**65**	**F**	**spor**	**55**	**1,160**	**4**	**41.9**	**7**	**he1; ne3; os10**	**Neg**	**ne4; th6; li7; os1**	**he1; ne3; th1; li5; os1**	+
19	58	F	spor	1,090	24	23	0.6	22	Neg	Neg	Neg	Neg	−/N
20	26	F	spor	35	261	N/A	0.9	−24	Neg	Neg	Neg	Neg	−/N
21	79	M	spor	144	1,758	13	664.8	12	N/P	ne2; ab1	ne1; th3; li1; ab2	ne1; th2; li1; ab3	−/N

*Patients who died of their disease.

Patients in boldface type are patients with a short calcitonin doubling time.

Spor = sporadic medullary thyroid cancer; MEN = multiple endocrine neoplasia; CgA = chromogranin A, reference level < 100 ug/L; calcitonin reference level < 12 ng/L; CEA = carcinoembryogenic antigen, reference level < 5 ug/L; Neg = negative; N/P = not performed; N/A = not applicable.

Imaging regions: he = head; ne = neck; th = thorax; li = liver; ab = abdomen; os = ossal. The number after the region denotes the number of lesions for that region.

Imaging performance: − = no added value to conventional; + = more lesions detected; ++ = ^{18}F-DOPA PET only positive imaging modality; — = ^{18}F-DOPA PET inferior; Y =imaging results have been cytologically confirmed; N = no histologic or cytologic confirmation has been made.

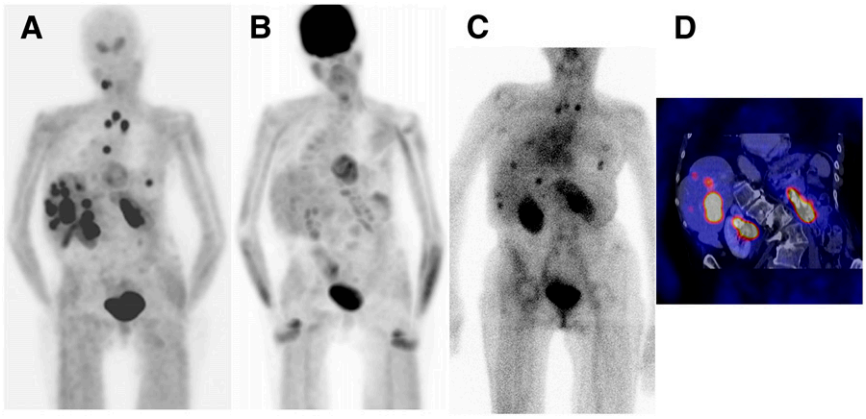

FIGURE 1. Patient 5: 68-y-old female patient with a MEN 2a–related metastasized recurrent MTC. Her calcitonin doubling time was 91 mo (calcitonin, 27,190 ng/L) and her CEA doubling time was 151 mo (CEA, 1,460 μg/L). (A) ^{18}F-DOPA PET shows the largest number of lesions, located in neck, upper mediastinum, left thorax, liver, and skeleton. (B) ^{18}F-FDG PET shows only physiologic uptake but no tumor lesions. (C) DMSA-V shows lesions in upper mediastinum, left thorax, liver, and skeleton, although with much smaller number of lesions. (D) ^{18}F-DOPA PET/CT fusion slice shows liver lesions.

These findings suggest better tumoral ^{18}F-FDG than ^{18}F-DOPA uptake in this subgroup with rapidly growing tumors.

Comparison of Imaging with CEA

CEA levels (median, 11.9 μg/L; range, 0.5–2,209.5 μg/L) were elevated in 14 patients (68%). In these patients, ^{18}F-DOPA PET was positive in 11 patients (2-sided $P = 0.0176$ for comparison of positive ^{18}F-DOPA PET results and elevated CEA), CT or MRI was positive in 6 patients (2-sided $P = 0.064$ for comparison of positive CT or MRI results and elevated CEA), DMSA-V was positive in 3 patients, and ^{18}F-FDG PET was positive in 3 patients. In 2 patients with elevated CEA (patients 1 and 15), imaging yielded no positive scan results. Of the 7 patients with normal CEA, 1 patient (patient 14) had numerous lesions (and elevated calcitonin) and 1 patient (patient 10) showed 1 tumor-positive lesion on ^{18}F-DOPA PET. CEA doubling time was generally in agreement with calcitonin doubling time.

Clinical Outcome

The 3 patients (patients 2, 12, and 18) who died after entering the study were characterized by short calcitonin (<12 mo) and CEA (<15 mo) doubling times. From our imaging results, these patients had extensively metastasized disease.

TABLE 2
Patient-Based Analysis

Imaging modality (performed on *n* patients)	No. of patients with positive lesions	Mean no. of lesions per patient (range)
CT or MRI ($n = 18$)	7	4.7 (0–18)
DMSA-V ($n = 18$)	5	1.1 (0–13)
^{18}F-FDG PET ($n = 17$)	4	1.6 (0–18)
^{18}F-DOPA PET (21)	13	4.6 (0–21)

On the basis of the inclusion criteria, all patients were considered positive for tumor. Sensitivities for patient-based analysis were calculated using total number of patients scanned per imaging modality as reference.

In 4 patients, surgery was performed on the basis of ^{18}F-DOPA PET findings. Before surgery, ^{18}F-DOPA PET images were fused with MR images for optimal anatomic localization. ^{18}F-DOPA PET findings were histopathologically confirmed in 4 cases. In all patients, calcitonin and CEA levels dropped after surgery but did not return to within the normal range. However, in 3 of these patients, these markers are rising again and, in 1 of these 3 patients, the calcitonin doubling time now is <12 mo.

DISCUSSION

Our results show that ^{18}F-DOPA PET improves staging in patients with biochemically suspected relapse or residual MTC. ^{18}F-DOPA PET detects more tumor-positive regions and lesions than CT or MRI, DMSA-V, and ^{18}F-FDG PET separately. Even when the results of CT or MRI, DMSA-V, and ^{18}F-FDG PET are pooled, ^{18}F-DOPA PET detects a slightly larger number of lesions. In addition, this study shows that the chances of obtaining positive ^{18}F-DOPA PET and negative ^{18}F-FDG PET are higher in those with a more indolent course of disease, whereas ^{18}F-FDG is more frequently positive as well when the clinical course is more aggressive, reflected by a rapid increase in tumor marker. In addition, our data indicate that morphologic imaging methods sometimes are complementary to the other imaging methods used in our study.

Two small studies—a retrospective study of Beuthien-Baumann (*20*) and a prospective study of Hoegerle (*12*)—suggested a role for ^{18}F-DOPA PET in MTCs. In both studies only a lesion-based analysis was performed. Whereas Beuthien-Baumann et al. had only written results of morphologic imaging at their disposal (*19*), Hoegerle et al. were able to use morphologic data for their analysis (*13*). Both studies used biochemical data but did not use these to establish a measure for biologic tumor behavior or tumor progression.

In our study calcitonin and CEA doubling times improved our understanding of the conflicting results of ^{18}F-FDG and ^{18}F-DOPA PET that are sometimes encountered. It seems that shorter calcitonin and CEA doubling

TABLE 3
Region-Based and Lesion-Based Analysis

Analysis	CT or MRI	DMSA-V	^{18}F-FDG PET	^{18}F-DOPA PET	^{18}F-DOPA PET with CT
Positive regions					
Head	3	2	0	4	4
Neck	4	3	4	8	8
Thorax	2	0	2	6	6
Liver	4	1	3	8	8
Abdomen	0	1	1	3	3
Bone	4	2	2	4	4
Total	17 (52%, 33%–69%)	9 (33%, 16%–54%)	12 (48%, 28%–69%)	33 (89%, 74%–97%)	33 (89%, 74%–97%)
Positive lesions					
Head	3	4	0	4	8
Neck	7	6	7	13	13
Thorax	15	0	9	18	20
Liver	28	4	10	47	50
Abdomen	0	1	2	5	5
Bone	27	5	3	8	27
Total	80 (64%, 55%–72%)	20 (19%, 12%–26%)	31 (30%, 23%–39%)	95 (71%, 62%–78%)	119 (89%, 82%–94%)

Number of positive regions and lesions per modality are given. Sensitivities and confidence intervals are given only for the rows in which total results for region-based and lesion-based analysis are presented. Sensitivities were calculated using composite reference data limited to patients scanned with the indicated imaging modality.

times are associated with increased tumoral glucose metabolism and decreased tumoral ^{18}F-DOPA metabolism. This is in line with findings on other aggressive (dedifferentiated?) neuroendocrine tumors, such as small cell lung cancer and metastatic paraganglioma in patients with a SDHB gene mutation, in which ^{18}F-FDG PET has a very high sensitivity for the detection of tumor lesions, whereas more "specialized" tracers, such as ^{18}F-DOPA and ^{18}F-dopamine show only marginal tumoral uptake (*21,22*). It is important to distinguish between local disease recurrence, which may be surgically curable, and systemic disease, in which case the aim is palliation. Therefore, it is important to adequately stage patients with MTC. ^{18}F-DOPA PET can provide a better understanding of tumor load—local as well as systemic disease—and can support the clinical decision in these patients with often slowly progressive tumors. For the control of local recurrent disease, clearance of lymph node metastases by systematic dissection may provide local control in the neck and mediastinum (*5–7,23,24*) and may prevent tracheal and esophageal invasion because of tumor infiltration (*25,26*). Local recurrent disease indisputably requires systematic lymph node dissection (*6,7,27*). There is still controversy on the treatment of metastasized disease. After apparent curative surgery for primary tumors, patients with persistent hypercalcitoninemia may have a 10-y survival of around 65% (*3,28*). However, for local disease control, dissection of the central and both lateral lymph node compartments of the neck may still have a role, but more accurate knowledge of both the number and the localization of the metastases can be helpful in the decision of whether to perform surgery. When only one distant lymph node compartment (either the contralateral side of the neck or the mediastinum) is involved, there is a 10% chance of cure (*29*).

Defining the gold standard for imaging studies in which new tracers may yield better results than the commonly used imaging methods is a difficult problem. Therefore, we choose to use a gold standard consisting of the combined data from all imaging modalities together (*18*). Because patients with MTC have a good life expectancy and undergo regular imaging to assess possible tumor growth, it was ethically not justifiable to try to verify all newly detected lesions. However, in 4 patients who did undergo surgery as a consequence of positive ^{18}F-DOPA PET findings, the detected lesions were resected and histologically confirmed to be tumor positive.

Combining multiple imaging modalities yields the best results for the detection of recurrent MTC. Morphologic imaging is important for accurate anatomic localization of MTC lesions. In our study, we did not have combined PET/CT available; therefore, we performed software-based rigid fusion of conventional imaging methods with PET to achieve a more accurate localization. Also, in this study, CT or MRI had excellent lesion visualization properties and often demonstrated lesions that were less evident on PET and vice versa. In addition, the combination of PET and CT by fusion software decreases reader uncertainties in deciding whether a lesion is "real" in this study, although it is difficult to "catch" that effect in numbers. Combined PET/CT will offer the best of both worlds and may become the diagnostic imaging procedure of choice in MTC (1-stop shop).

Establishing a perfect gold standard is difficult in every diagnostic accuracy study. As in our case, newer diagnostic methods can be far better than current standard methods

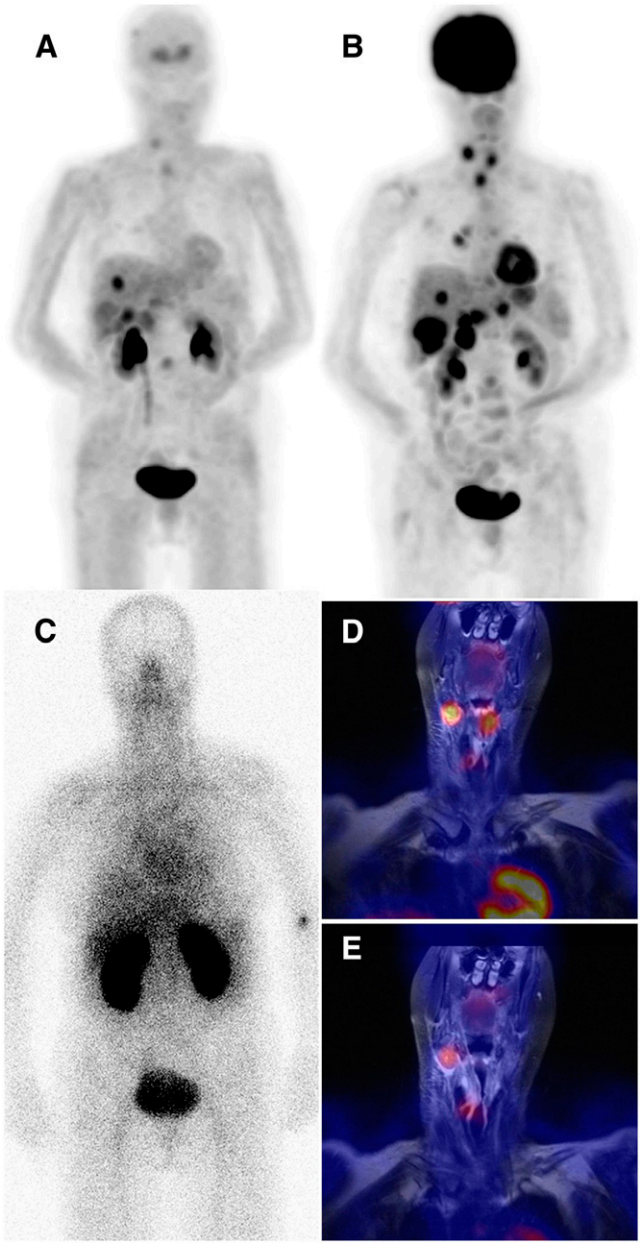

FIGURE 2. Patient 18: 65-y-old female patient with sporadic MTC. Her calcitonin doubling time was 4 mo (calcitonin, 1,160 ng/L) and her CEA doubling time was 7 mo (CEA, 41.9 μg/L). (A) ^{18}F-DOPA PET projection image shows lesions with vague uptake in skull, neck, liver, and spine but also lesions with intense uptake. (B) ^{18}F-FDG PET shows many more lesions with intense uptake in the neck, mediastinum, liver, and spine. (C) DMSA-V scan shows no lesions. (D) ^{18}F-FDG PET/MRI fusion slice shows 3 lesions in neck. However, on ^{18}F-DOPA PET/MRI fusion (E), only 2 lesions show vague uptake. Different lesional uptake within 1 patient most likely illustrates different degrees of tumor dedifferentiation within 1 patient.

and detect many unknown lesions, which can never all be verified using cytologic or histologic analysis. Whenever possible, we verified new findings, but also used common sense and assumed that—when several lesions were verified—other lesions with identical and unequivocal uptake of this specific tracer in the same patient could also be regarded as true tumor lesions. Some dependency of PET results and our composite reference standard is present in this study. However, this dependency is also present for CT and somatostatin receptor scintigraphy. Still, our sensitivity values should be regarded with some caution (*18,30*).

There is an ongoing search for new tracers for MTC, as the problem of increased tumor marker and negative imaging is experienced in many centers. Even in this study, with extensive diagnostic tests, 5 of 21 (24%) of the patients remained negative on all performed tests. Because not all imaging modalities were available for the patients, the value of ^{18}F-FDG PET in progressive disease has been underexposed; thus, more data on the difference in ^{18}F-DOPA and ^{18}F-FDG PET uptake are necessary to prove the value in patients with progressive MTC.

New approaches, such as gastrin receptor scintigraphy, are promising because of the high expression of the cholecystokinin 2 receptor in MTCs (*31,32*). However, because of the variation in biologic behavior of MTC, the future will reveal what the best imaging approach for these tumors will be. Very likely individual tailoring with different imaging methods based on biologic behavior will be necessary for optimal staging of MTC in patients.

CONCLUSION

^{18}F-DOPA PET is superior to ^{18}F-FDG PET and DMSA-V scintigraphy in staging of MTC and is probably the best noninvasive staging method yet available. A decrease in serum calcitonin doubling time and a shift from ^{18}F-DOPA PET positivity to more ^{18}F-FDG PET indicates aggressive tumor behavior and may support the choice for systemic therapy.

REFERENCES

1. Kebebew E, Ituarte PH, Siperstein AE, Duh QY, Clark OH. Medullary thyroid carcinoma: clinical characteristics, treatment, prognostic factors, and a comparison of staging systems. *Cancer.* 2000;88:1139–1148.
2. Orlandi F, Caraci P, Mussa A, et al. Treatment of medullary thyroid carcinoma: an update. *Endocr Relat Cancer.* 2001;8:135–147.
3. de Groot JW, Plukker JT, Wolffenbuttel BH, et al. Determinants of life expectancy in medullary thyroid cancer: age does not matter. *Clin Endocrinol (Oxf).* 2006;65:729–736.
4. Ong SC, Schoder H, Patel SG, et al. Diagnostic accuracy of ^{18}F-FDG PET in restaging patients with medullary thyroid carcinoma and elevated calcitonin levels. *J Nucl Med.* 2007;48:501–507.
5. Moley JF, DeBenedetti MK. Patterns of nodal metastases in palpable medullary thyroid carcinoma: recommendations for extent of node dissection. *Ann Surg.* 1999;229:880–887.
6. Scollo C, Baudin E, Travagli JP, et al. Rationale for central and bilateral lymph node dissection in sporadic and hereditary medullary thyroid cancer. *J Clin Endocrinol Metab.* 2003;88:2070–2075.
7. de Groot JW, Links TP, Sluiter WJ, et al. Locoregional control in patients with palpable medullary thyroid cancer: results of standardized compartment-oriented surgery. *Head Neck.* 2007;29:857–863.
8. Cohen EG, Shaha AR, Rinaldo A, Devaney KO, Ferlito A. Medullary thyroid carcinoma. *Acta Otolaryngol.* 2004;124:544–557.
9. de Groot JW, Links TP, Jager PL, Kahraman T, Plukker JT. Impact of ^{18}F-fluoro-2-deoxy-D-glucose positron emission tomography (FDG-PET) in patients with biochemical evidence of recurrent or residual medullary thyroid cancer. *Ann Surg Oncol.* 2004;11:786–794.

10. Khan N, Oriuchi N, Higuchi T, Endo K. Review of fluorine-18-2-fluoro-2-deoxy-D-glucose positron emission tomography (FDG-PET) in the follow-up of medullary and anaplastic thyroid carcinomas. *Cancer Control.* 2005;12:254–260.
11. Uchino H, Kanai Y, Kim DK, et al. Transport of amino acid-related compounds mediated by L-type amino acid transporter 1 (LAT1): insights into the mechanisms of substrate recognition. *Mol Pharmacol.* 2002;61:729–737.
12. Hoegerle S, Altehoefer C, Ghanem N, et al. ^{18}F-DOPA positron emission tomography for tumour detection in patients with medullary thyroid carcinoma and elevated calcitonin levels. *Eur J Nucl Med.* 2001;28:64–71.
13. Gourgiotis L, Sarlis NJ, Reynolds JC, et al. Localization of medullary thyroid carcinoma metastasis in a multiple endocrine neoplasia type 2A patient by 6-[^{18}F]-fluorodopamine positron emission tomography. *J Clin Endocrinol Metab.* 2003;88:637–641.
14. de Vries EF, Luurtsema G, Brussermann M, Elsinga PJ, Vaalburg W. Fully automated synthesis module for the high yield one-pot preparation of 6-[^{18}F]-fluoro-L-DOPA. *Appl Radiat Isot.* 1999;51:389–419.
15. Brown WD, Oakes TR, DeJesus OT, et al. Fluorine-18-fluoro-L-DOPA dosimetry with carbidopa pretreatment. *J Nucl Med.* 1998;39:1884–1891.
16. Ishikawa T, Dhawan V, Chaly T, et al. Fluorodopa positron emission tomography with an inhibitor of catechol-O-methyltransferase: effect of the plasma 3-O-methyldopa fraction on data analysis. *J Cereb Blood Flow Metab.* 1996;16:854–863.
17. Orlefors H, Sundin A, Lu L, et al. Carbidopa pretreatment improves image interpretation and visualisation of carcinoid tumours with ^{11}C-5-hydroxytryptophan positron emission tomography. *Eur J Nucl Med Mol Imaging.* 2006;33:60–65.
18. Koopmans KP, de Vries EG, Kema IP, et al. Staging of carcinoid tumours with ^{18}F-DOPA PET: a prospective, diagnostic accuracy study. *Lancet Oncol.* 2006; 7:728–734.
19. Miyauchi A, Onishi T, Morimoto S, et al. Relation of doubling time of plasma calcitonin levels to prognosis and recurrence of medullary thyroid carcinoma. *Ann Surg.* 1984;199:461–466.
20. Beuthien-Baumann B, Strumpf A, Zessin J, Bredow J, Kotzerke J. Diagnostic impact of PET with (^{18}F-FDG, ^{18}F-DOPA and 3-O-methyl-6-[^{18}F]fluoro-DOPA in recurrent or metastatic medullary thyroid carcinoma. *Eur J Nucl Med Mol Imaging.* 2007;34:1604–1609.
21. Jacob T, Grahek D, Younsi N, et al. Positron emission tomography with [^{18}F]FDOPA and [^{18}F]FDG in the imaging of small cell lung carcinoma: preliminary results. *Eur J Nucl Med Mol Imaging.* 2003;30:1266–1269.
22. Timmers HJ, Kozupa A, Chen CC, et al. Superiority of fluorodeoxyglucose positron emission tomography to other functional imaging techniques in the evaluation of metastatic SDHB-associated pheochromocytoma and paraganglioma. *J Clin Oncol.* 2007;25:2262–2269.
23. Gimm O, Ukkat J, Dralle H. Determinative factors of biochemical cure after primary and reoperative surgery for sporadic medullary thyroid carcinoma. *World J Surg.* 1998;22:562–567.
24. Machens A, Holzhausen HJ, Dralle H. Prediction of mediastinal lymph node metastasis in medullary thyroid carcinoma. *Br J Surg.* 2004;91:709–712.
25. Kebebew E, Kikuchi S, Duh QY, Clark OH. Long-term results of reoperation and localizing studies in patients with persistent or recurrent medullary thyroid cancer. *Arch Surg.* 2000;135:895–901.
26. Machens A, Hinze R, Lautenschlager C, Thomusch O, Dralle H. Thyroid carcinoma invading the cervicovisceral axis: routes of invasion and clinical implications. *Surgery.* 2001;129:23–28.
27. Moley JF, DeBenedetti MK. Patterns of nodal metastases in palpable medullary thyroid carcinoma: recommendations for extent of node dissection. *Ann Surg.* 1999;229:880–887.
28. Bergholm U, Bergstrom R, Ekbom A. Long-term follow-up of patients with medullary carcinoma of the thyroid. *Cancer.* 1997;79:132–138.
29. Machens A, Holzhausen HJ, Dralle H. Contralateral cervical and mediastinal lymph node metastasis in medullary thyroid cancer: systemic disease? *Surgery.* 2006;139:28–32.
30. Hicks RJ, Ware RE, Lau EW. PET/CT: will it change the way that we use CT in cancer imaging? *Cancer Imaging.* 2006;31(suppl):S52–S62.
31. Behr TM, Jenner N, Radetzky S, et al. Targeting of cholecystokinin-B/gastrin receptors in vivo: preclinical and initial clinical evaluation of the diagnostic and therapeutic potential of radiolabelled gastrin. *Eur J Nucl Med.* 1998;25:424–430.
32. Gotthardt M, Behe MP, Beuter D, et al. Improved tumour detection by gastrin receptor scintigraphy in patients with metastasised medullary thyroid carcinoma. *Eur J Nucl Med Mol Imaging.* 2006;33:1273–1279.

JNM The Journal of NUCLEAR MEDICINE

^{18}F-Dihydroxyphenylalanine PET in Patients with Biochemical Evidence of Medullary Thyroid Cancer: Relation to Tumor Differentiation

Klaas P. Koopmans, Jan Willem B. de Groot, John T.M. Plukker, Elisabeth G.E. de Vries, Ido P. Kema, Wim J. Sluiter, Pieter L. Jager and Thera P. Links

J Nucl Med. 2008;49:524-531.
Doi: 10.2967/jnumed.107.047720

The Journal of Nuclear Medicine is published monthly.
SNMMI | Society of Nuclear Medicine and Molecular Imaging
1850 Samuel Morse Drive, Reston, VA 20190.
(Print ISSN: 0161-5505, Online ISSN: 2159-662X)

SNMMI SOCIETY OF NUCLEAR MEDICINE AND MOLECULAR IMAGING